HIGHLY MANEUVERABLE AIRCRAFT TECHNOLOGY

Dwain A. Deets
Chief, Systems Analysis Branch
NASA Hugh L. Dryden Flight Research Center
P. O. Box 273
Edwards, California 93523
USA

and

Carl A. Crother
HiMAT Project Engineer, Flight Controls
Rockwell International, Los Angeles Division
International Airport
Los Angeles, California 90009
USA

SUMMARY

A remotely piloted research vehicle (RPRV) with active controls has been designed to develop highly maneuverable aircraft technologies (HiMAT). The HiMAT RPRV is the central element in a new method to bring advanced aircraft technologies to a state of readiness. The RPRV is well into the construction phase, with flight test evaluations planned.

The closely coupled canard-wing vehicle includes relaxed static stability, direct force control, and a digital active control system. Nonlinearities in the aerodynamics led to unusual demands on the active control systems. For example, the longitudinal static margin is 10-percent negative at low angles of attack, but increases to 30-percent negative at high angles of attack and low Mach numbers.

This paper discusses the design procedure followed and experiences encountered as they relate to the active control features. Emphasis is placed on the aspects most likely to be encountered in the design of a full-scale operational vehicle. In addition, a brief overview of the flight control system features unique to the RPRV operation is presented.

NOMENCLATURE

C_L	lift coefficient
C_m	pitching moment coefficient
$C_{m_{C_L}}$	$\frac{\partial C_m}{\partial C_L}$, pitching moment with respect to lift coefficient
C_n	yawing moment coefficient
C_{n_β}	$\frac{\partial C_n}{\partial \beta}$, yawing moment with respect to angle of sideslip, rad^{-1}
$C_{n_{\delta_r}}$	$\frac{\partial C_n}{\partial \delta_r}$, yawing moment with respect to rudder deflection, rad^{-1}
cg	center of gravity
$\bar{c}_w$	mean geometric and aerodynamic chord of the wing, m
HiMAT	highly maneuverable aircraft technology
h	altitude, m
K	gain
$K(\cdot)$	gain programmed as a function of $(\cdot)$
K_{n_Y}	lateral acceleration feedback gain to the rudder, deg/g
K_p	roll rate feedback to the antisymmetric elevons, sec
K_r	yaw rate feedback to the rudders, sec
LVDT	linear voltage differential transformer
M	Mach number
n_Y	lateral acceleration, g
n_Z	normal acceleration, g
PROM	programable read-only memory
p	angular velocity about the roll axis, deg/sec
q	angular velocity about the pitch axis, deg/sec
$\bar{q}$	dynamic pressure, N/m^2
RPRV	remotely piloted research vehicle
RSS	relaxed static stability
r	angular velocity about the yaw axis, deg/sec
s	Laplace variable
α	angle of attack, deg
α_ℓ	limit angle of attack, deg
β	angle of sideslip, deg
δ_a	aileron deflection, $\delta_{a_L} - \delta_{a_R}$, deg
δ_{a_p}	pilot's roll stick command, cm
δ_c	canard flap deflection, $\frac{\delta_{c_L} + \delta_{c_R}}{2}$, deg

$\delta_{c_t}(\cdot)$	canard flap trim input programed as a function of $(\cdot)$, deg
δ_e	elevator deflection, $\frac{\delta_{e_L} + \delta_{e_R}}{2}$, deg
δ_{e_p}	pilot's pitch stick command, cm
δ_f	elevon surface deflection, deg
δ_{f_a}	antisymmetrical elevon deflection, $\delta_{f_L} - \delta_{f_R}$, deg
δ_{f_s}	symmetrical elevon deflection, $\frac{\delta_{f_L} + \delta_{f_R}}{2}$, deg
δ_r	rudder deflection, deg
δ_{r_p}	pilot's rudder pedal command, cm

Subscripts:

com	command
L	left
R	right

INTRODUCTION

A subscale remotely piloted research vehicle (RPRV) has been designed as part of the highly maneuverable aircraft technology (HiMAT) program. The HiMAT RPRV design is the central element in a new method for bringing advanced aircraft technologies to a state of readiness. The method begins with a paper design of an aircraft incorporating the new technologies of interest. A subscale RPRV is then designed and built to demonstrate the advanced technologies in a flight environment. The first application of the method is in the high maneuverability areas incorporated in the HiMAT vehicle. An overview of the HiMAT RPRV in terms of the various new technology areas to be demonstrated is given in reference 1.

One of the new technology areas included in the HiMAT program is active controls. Although several functions are included under the active controls banner, relaxed static stability (RSS) and direct force control are the only functions included in the HiMAT design, because they offer the greatest potential for improved performance. RSS is applied to both the longitudinal and directional axes, although the longitudinal axis is substantially more dependent on active controls. Several studies, such as those described in references 2 and 3, have concluded that RSS benefits are highly dependent on configuration. The HiMAT vehicle, with a closely coupled canard-wing planform, represents a fighter configuration significantly different from the conventional wing-tail fighter configuration. In addition, the HiMAT vehicle has aeroelastic tailoring which, when combined with a construction technique that yields a more flexible structure, results in highly nonlinear aerodynamics. Thus, the application of RSS to this unconventional configuration offers the potential for an important advancement in the active controls technology base for fighter aircraft.

The NASA-sponsored HiMAT program has received the guidance and assistance of the United States Air Force, both in Washington, D.C., and at Wright-Patterson Air Force Base. Rockwell International is under contract to the NASA Dryden Flight Research Center (DFRC) to design and manufacture two vehicles. The HiMAT RPRV is currently in the construction phase at the Rockwell International, Los Angeles Division, facility; delivery of the first vehicle is planned for March 1978. Flight test evaluations are to be performed at the NASA DFRC following ground checkout.

This paper discusses the design procedure followed and experiences encountered as they relate to the active control features. Emphasis is placed on the aspects most likely to be encountered in the design of a full-scale aircraft of similar planform. Details of the resulting primary control laws are presented. An overview of the backup control laws and the implementation of the primary and backup systems is given, since they are unique to the RPRV operation.

HiMAT RPRV CONCEPT

The HiMAT RPRV concept is to use RPRV's to speed the technology transition from wind tunnel to flight and to reduce the cost of aeronautical experiments exercising new technology. The concept involves two distinct steps: the first is a design study of a full-scale airplane; the second is the design, manufacture, and flight test of a subscale RPRV.

Full-Scale Fighter Design

Three contractors performed conceptual design studies of a full-scale fighter aircraft employing synergistic combinations of new technologies. The maneuverability goal for the full-scale fighter aircraft was the ability to sustain an 8g turn at Mach 0.9 at an altitude of 9140 meters. The studies also included an assessment of the problems associated with demonstrating the technologies on a subscale RPRV.

The Rockwell design stresses the use of aerodynamic and structural technologies to obtain the high maneuverability. The design closely couples canard and wing, bringing the two lifting surfaces close together to develop a favorable interaction in their flow fields by way of a tailored total airplane span load distribution. This requires low drag at lift coefficients greater than 1.0.

Subscale RPRV

The subscale HiMAT RPRV to be used to demonstrate the new technologies in flight is a 0.44-scale version of the full-scale fighter aircraft. The maneuverability goal for the RPRV was the ability to sustain an 8g turn at Mach 0.9. An altitude of 7620 meters was selected to effectively match the wing loading of the full-scale aircraft. Figure 1 is a three-view drawing of the HiMAT RPRV with control surfaces indicated. The canard flaps are used either symmetrically, for longitudinal control, or antisymmetrically, for direct side force control. The ailerons and elevators are used for roll and pitch control, respectively. The elevons may be commanded antisymmetrically

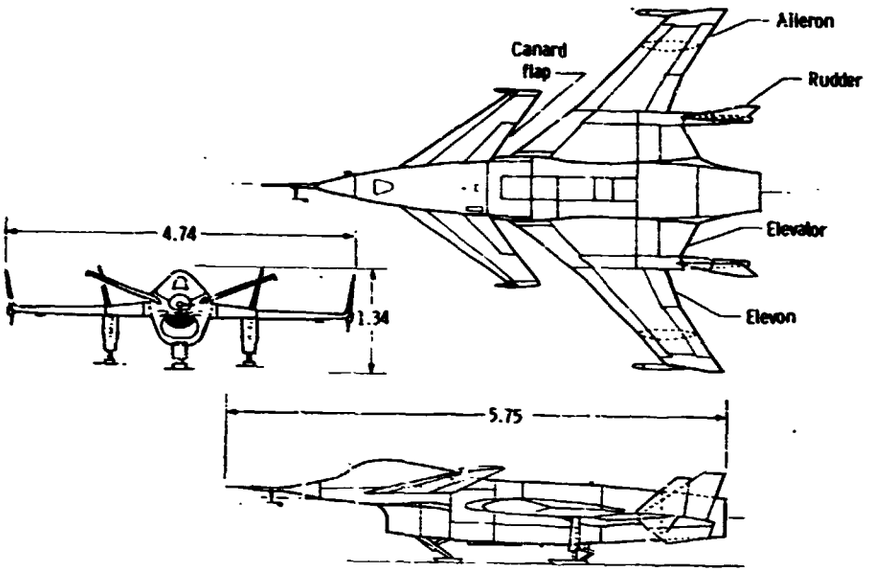

Figure 1. Three-view drawing of HiMAT RPRV. Dimensions are in meters.

for roll control or symmetrically for pitching moment control. The rudders may be commanded collectively for yawing moment control or differentially as a speed brake. The 1500-kilogram vehicle is to be air-launched from a B-52 airplane and will carry 270 kilograms of fuel for the J85-21 engine. The vehicle will be landed horizontally on a dry lakebed under primary control of a ground-based pilot using controls and instrument displays typical of those used in conventional fighter aircraft, as well as a television display generated from an onboard, forward-looking television camera.

Several features of the full-scale fighter design were not included in the RPRV. For example, a two-dimensional nozzle was not included because of cost constraints. Blended wing-body and canard strakes were not included because the two-dimensional nozzle would have been necessary to trim out the resulting high angle-of-attack pitching moment characteristics. A low cost approach was used whenever possible. In some cases, low cost could be achieved by using methods unique to an RPRV operation and without compromises in performance. In other cases, some compromises in performance were necessary. Some of the low cost methods and the effects on performance are detailed below.

Limited wind tunnel data base

Although computerized aerodynamic methods were preferred as a configuration development design tool, none of the methods completely accounted for the entire configuration (body, canard, wing, and winglet). Wind tunnel tests were consequently a necessary ingredient in the aerodynamic configuration development. However, in keeping with the low cost approach, the amount of testing was considerably less than that usually expended for a refined manned fighter aircraft. Only 800 hours of wind tunnel tests were run before initiating fabrication of the HiMAT vehicle. By comparison, approximately 2000 hours are required for a typical prototype manned airplane (for example, 1940 hours for the YF-16 airplane) and approximately 10,000 hours for a fully refined airplane (12,000 hours for the F-14 airplane).

Low cost elements

An important aspect in achieving low cost in the subscale RPRV was the modular design of the control surface actuators (canards, ailerons, elevons, elevators, and rudders). The combination of common components led to a variety of servoactuator implementations, namely dual tandem, single, and single tandem. This was cost effective in design and fabrication, minimized spare part requirements, and will facilitate future configuration changes.

While all performance requirements were met with the modular actuators, several compromises were made in the system's functional capability to accrue additional cost savings. Although an all-movable canard would have been necessary to obtain the incremental 1g design goal for direct lift, a less effective and less costly canard flap was used. Despite falling 50-percent short of the design goal, the direct lift capabilities of the closely coupled canard configuration can still be demonstrated.

In some instances, manual configuration changes must be made on the ground between flights of the RPRV in order to demonstrate features of the full-scale fighter aircraft. The wing and canard leading edges, rather than being continuously variable as in the full-scale fighter aircraft, must be manually changed to one of two distinct settings. One setting is denoted "maneuver wing"; the other is denoted "cruise wing." The direct force canard controls, rather than providing an arbitrary mixture of direct lift and direct side force, must be selected for one or the other function by the ground-based pilot.

Ground facility

Another feature of the RPRV operation that reduces program costs is the ground facility, which contains a cockpit with controls and displays typical of conventional fighter aircraft. A general purpose minicomputer is also available for mechanizing a control system on the ground. Figure 2 illustrates the arrangement between the vehicle and the ground facility. The pilot and the ground-based minicomputer send signals to the vehicle control surface

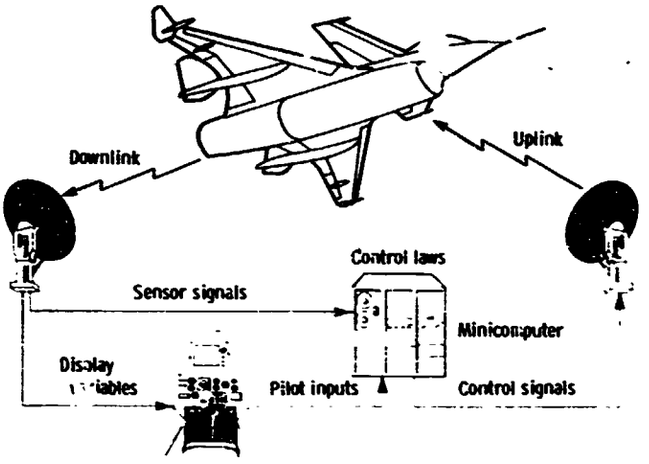

Figure 2. Conceptual layout of RPRV operation with ground facility.

actuators through the uplink system. Resultant vehicle motions are then sensed and sent back to the pilot and the control system computer by way of the downlink, thus providing closed-loop control of the vehicle. Reference 4 provides additional details on this operation.

A high level FORTRAN compiler is available for the ground-based minicomputer, providing an order-of-magnitude savings in coding and software validation costs as compared with flight computer software.

Hardware cost savings are possible because the facility is already in existence and the facility equipment costs are divided among a number of programs.

Reliability specification

The system reliability specification imposed on the HiMAT RPRV was less demanding than that appropriate for manned aircraft but more demanding than that normally associated with a drone. The contract specification that "no single failure shall cause loss of the vehicle" was imposed to protect the vehicle following a first failure, but protection against subsequent failures was not required. Consequently, the resulting system configuration is considerably different from what one would expect for an active control system in a manned aircraft.

The primary system, which uses the ground-based minicomputer, is functionally similar to that of a full-scale fighter aircraft with respect to the control laws. It is a simplex system with in-line monitoring. The backup system is in no way similar to that appropriate for a manned vehicle. It is a semiautomatic system that must provide safe return and landing capability, independent of the ground facility. An alternate command station in a chase airplane is used to make autopilot-type commands typical of drone operation. An onboard, microprocessor-based control system provides the necessary autopilot functions for stabilization, orbit, cruise at wings level, and approach and flare.

INTEGRATED ACTIVE CONTROLS DESIGN

Design Procedure

As in conventional airplane design procedures, the active controls design involved an iterative process. Figure 3 illustrates one cycle of the process. A set of requirements and a startup configuration were used to

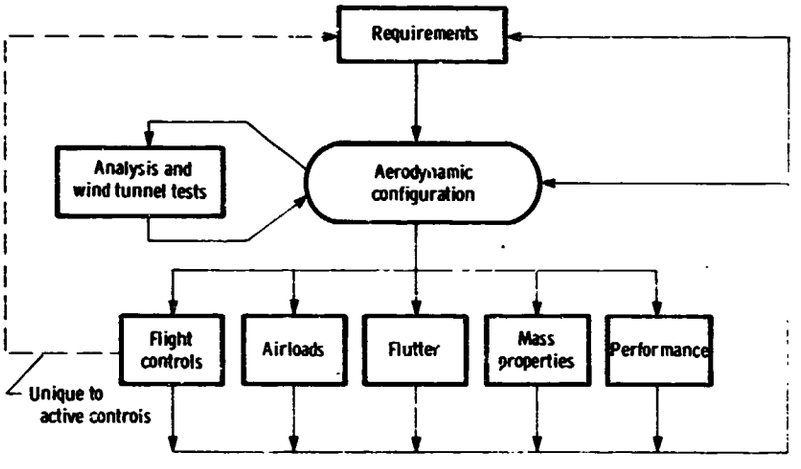

Figure 3. One cycle of iterative integrated design process.

define wind tunnel models and analytical aerodynamic models. Test results from these models formed the basis of a revised aerodynamic configuration and provided the necessary data to update or begin the various support activities, including flight control design, airload and flutter analysis, mass properties definition, and performance analysis. Results of the various analyses resulted in either confirmation of an acceptable configuration or an adjustment to the requirements that governed the subsequent iteration. The dashed line in the figure represents the need for early definition of control requirements prior to the iteration cycle. It corresponds to the aerodynamic configuration developer's asking the controls engineer, "How much control power is needed?" The controls engineer responds with a question: "What do I have to stabilize?"

It is interesting to note that the function of assuring the final level of adequate stability and control was performed by the flight controls engineers, rather than by the aerodynamics engineers as is the usual case with conventional airplane designs. In addition, the flight controls group was involved in the configuration development from the start rather than being consulted later in the design process.

With the exception of the need to establish control power sizing requirements before sufficient information was available to state such requirements, and the transfer of stability and control responsibility, the design process was rather standard. Although the flight controls engineers received the aerodynamic characteristics corresponding to the most recent configuration data set, the flexibility corrections were not available until the new iteration on airloads was completed. Because the flutter analysis lagged behind the other analyses, its iteration cycle was longer.

Design Experiences

Three aspects of the configuration development stand out as unique to the active controls philosophy in the design. Two of these involved relaxed static stability; the third, direct force control.

Relaxed longitudinal static stability

In the early configuration development, the major problem related to relaxed static stability was the determination of control power requirements. Initially, based on advanced manned strategic aircraft design experience (ref. 5), 10-percent negative longitudinal static margin was selected as a limit for the rigid airplane. This limit was later increased to 15-percent negative based on the following rationale.

The landing condition in a wind gust was found to be critical. A ground rule was established that 20-percent control surface travel should be available for stability augmentation, after accounting for trimming to the landing condition and encountering a wind shear of reasonable intensity. The wing trailing edge pitch control surfaces (elevator and symmetric elevons) have a 30° trailing edge down limit; therefore, a deflection of no more than 25° trailing edge down could be allotted for trim plus wind shear. For a landing speed of 80 meters per second and a 15-percent negative static margin, a wind shear equivalent to a $\Delta\alpha$ of 5.7° or a Δn_z of 0.4g could be tolerated under the above restrictions. This was considered a reasonable combination of landing speed and wind shear.

At higher angles of attack, a sharp nonlinearity in $C_{m_{C_L}}$ actually increased the static margin to more than 30-percent negative at some low subsonic flight conditions. To illustrate the degree of instability, including the effects of cg changes and flexibility corrections, figure 4 shows C_L as a function of C_m for the cruise wing at Mach numbers of 0.9, 0.7, and 0.2.

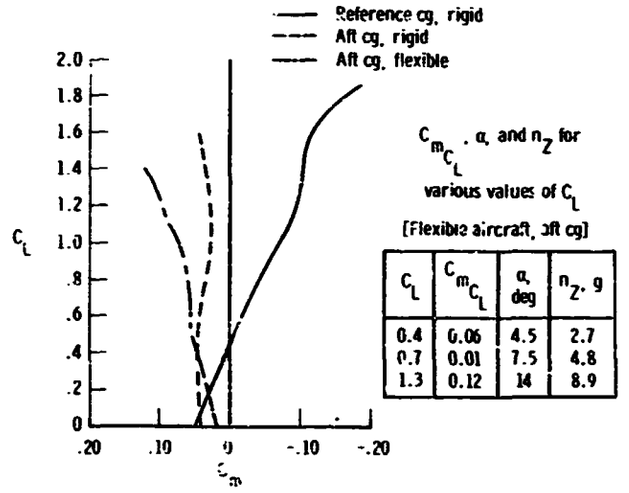

$C_{m_{C_L}}$, α, and n_Z for various values of C_L
[Flexible aircraft, aft cg]

C_L	$C_{m_{C_L}}$	α, deg	n_Z, g
0.4	0.06	4.5	2.7
0.7	0.01	7.5	4.8
1.3	0.12	14	8.9

(a) Mach 0.9, h = 9140 meters.

Figure 4. Longitudinal stability of cruise wing HiMAT vehicle.

The data for Mach 0.9 are presented in figure 4(a). The curves show the flexibility effects for the flight condition at an altitude of 9140 meters with the indicated instability. The rigid curve corresponds to the reference cg position (0-percent $\bar{c}_w$) and is obviously stable. With the cg at 10-percent $\bar{c}_w$, which corresponds to the farthest aft cg position, the curve shows essentially neutral stability. The inserted table presents the magnitude of instability for several values of C_L. In addition, the approximate α and n_Z values corresponding to each C_L value are listed for a weight of 1390 kilograms. The instabilities shown range from 0.06 at a C_L of 0.4 to 0.12 at a C_L of 1.3 ($n_Z \approx 8.9$g).

Figure 4(b) illustrates similar data for the Mach 0.7 condition at an altitude of 9140 meters. The instabilities range from 0.11 to 0.21 for the C_L values shown. The Mach 0.2 data are presented in figure 4(c) and the cg effects are shown. (Flexibility effects are negligible at this Mach number.) For an altitude of 7620 meters, the instabilities range from 0.10 to 0.31. At such extremely negative stability levels, the pitch control surface will always reach its limit at some sufficiently large angle of attack; thus, stability augmentation will be lost. It should be noted that control power saturation does not occur in the maneuver portion of the HiMAT RPRV flight envelope and hence, does not restrict the demonstration of the highly maneuverable capabilities. However, to preserve vehicle control during low dynamic pressure, high angle-of-attack flight, an angle-of-attack limiter was planned for incorporation in the control system.

Some penalties were incurred because of the RSS system requirements. Larger hinge moments, resulting in larger actuators, were required. This necessitated going outside the wing mold lines on the RPRV and probably would cause a similar problem on a full-scale fighter aircraft. Although not quantified, the weight for the larger hydraulic system was greater than that required for a conventional design.

Relaxed directional static stability

As in the longitudinal RSS design, incorporation of RSS in the directional axis required early estimates of control power requirements. Initially, a goal of neutral directional stability based on a rigid airplane was established. Any further decrease in the stability level was not warranted on the basis of performance improvement alone. Even at neutral stability, an initial estimate of the control power required to provide adequate directional stability was needed. The controls engineers decided to state their requirement in terms of $C_{n_{\delta_r}}/C_{n_\beta}$ evaluated at an angle of sideslip of 2°. $C_{n_{\delta_r}}$ is negative and C_{n_β} is normally positive, so the

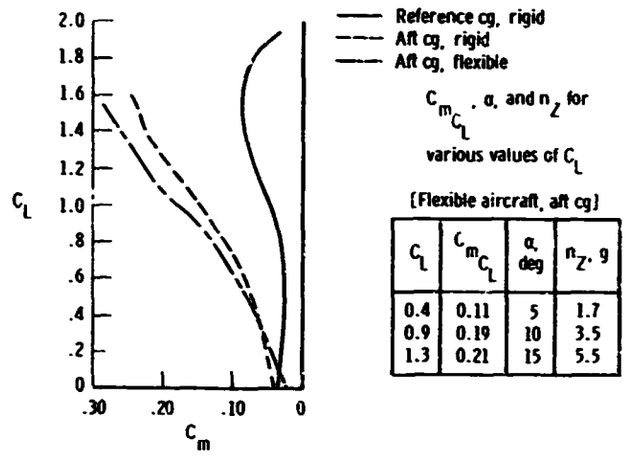

(Flexible aircraft, aft cg)

C_L	$C_{m_{C_L}}$	α, deg	n_z, g
0.4	0.11	5	1.7
0.9	0.19	10	3.5
1.3	0.21	15	5.5

(b) Mach 0.7, h = 9140 meters.

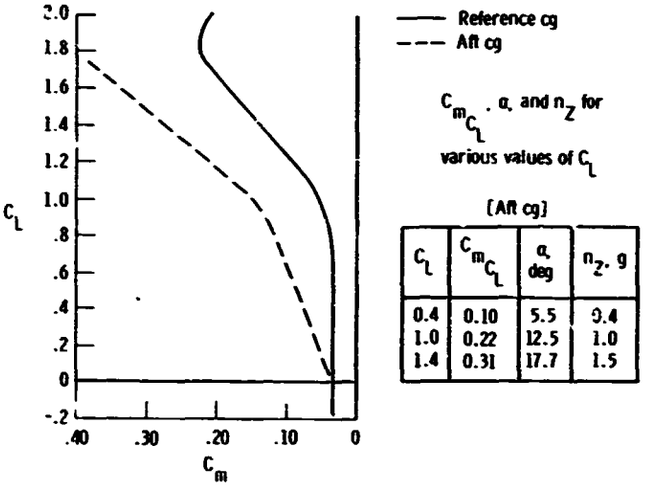

(Aft cg)

C_L	$C_{m_{C_L}}$	α, deg	n_z, g
0.4	0.10	5.5	0.4
1.0	0.22	12.5	1.0
1.4	0.31	17.7	1.5

(c) Mach 0.2.

Figure 4. Concluded.

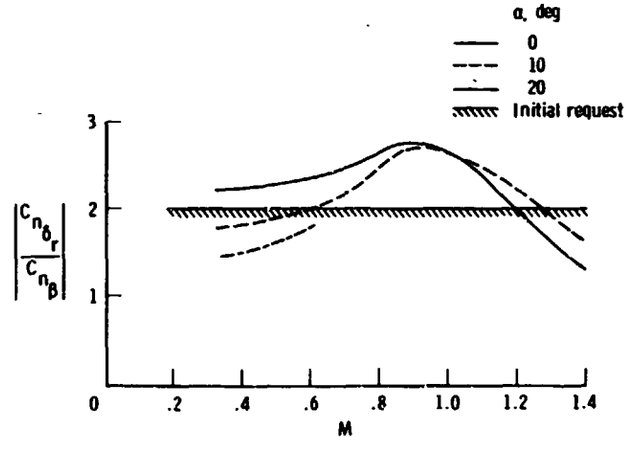

Figure 5. Ratio of yawing moment due to rudder deflection to yawing moment due to angle of sideslip as a function of Mach number.

$C_{n_{\delta_r}}/C_{n_\beta}$ ratio is negative. For a neutrally stable airplane, C_{n_β} is zero and the $C_{n_{\delta_r}}/C_{n_\beta}$ ratio goes to infinity. In other words, very little rudder effectiveness is needed to stabilize a neutrally stable airplane in the directional axis. The control power requested by the controls group and based on the rigid airplane was ultimately about 50-percent higher than that provided. Figure 5 shows the wind tunnel values for a range of Mach numbers and angles of attack as compared with the initial request. Even though the control power is below the initial request, simulation studies have indicated it is adequate.

The flexibility effects played a major role in the design. Wind tunnel data, corrected for flexibility and cg effects, predict a nonlinearity in C_{n_β} (fig. 6), resulting in negative directional stability to 1.5° of sideslip. This nonlinearity is caused by the flexible characteristics of the vertical tails and the winglets. Because these surfaces are aft of the cg, the flexibility effects tend to negate the directional stability the surfaces would otherwise provide.

The tendency to trim directionally at nonzero angles of sideslip would have been undesirable without active controls. However, with active controls it could be assumed that the control system could be programed to remove any such tendency.

Direct force control

Direct force control is provided in two axes. Normal force is provided by the direct lift control system; side force is provided by the direct side force control system.

The direct lift control system utilizes the canard flap, in conjunction with the wing trailing edge surfaces, to provide pure lift. A canard flap normally produces nose up pitching moment as well as direct lift. However, with the HiMAT RPRV, the symmetric elevons and elevators are deflected to a trailing edge down position by the active control system to trim out the pitching moment. This effectively increases the wing camber, which increases the total vehicle lift. Interestingly, the canard flap lift effectiveness reverses at dynamic pressures above 30,000 N/m^2 because the canard flap trailing edge down deflection causes downwash, which reduces the angle of attack at the wing, thereby reducing lift. However, a positive pitching moment is still generated, which results in the same downward deflections of the wing trailing edge surfaces through the active control system, and hence, direct lift as before.

Direct side force is achieved by deflection of the antisymmetric canard flap in conjunction with the rudders and antisymmetric wing trailing edge surfaces. To generate the side force with the canard flaps, dihedral was required in the canards. The dihedral ahead of the cg was destabilizing directionally. The winglet ventrals were added to return the rigid airplane to neutral directional stability at the 9-percent $\bar{c}_w$ reference cg.

PRIMARY CONTROL LAWS

The primary control laws were designed to meet the basic military handling qualities

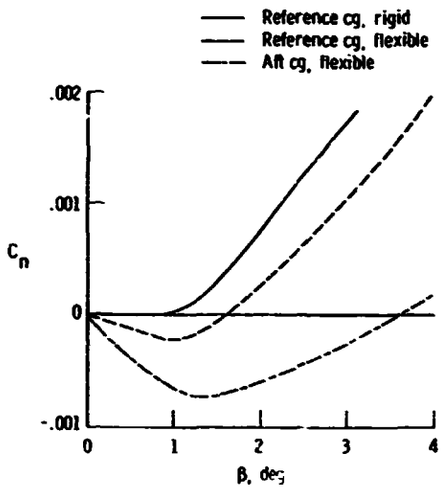

Figure 6. Yawing moment in stability axis system as a function of angle of sideslip. Mach 0.9; h = 3050 meters.

specification from MIL SPEC-F-8785B(ASG) (ref. 6). Therefore, the relationship between the control law design and the configuration development for the HiMAT RPRV should have been similar to the relationship for a full-scale manned vehicle. The design philosophy chosen is discussed, and the longitudinal and lateral-directional primary control laws are described.

Design Philosophy

The most significant assumption was that a full-time digital fly-by-wire system would be available to connect the pilot's inputs and a standard set of motion sensors to all the control surfaces. The digital computer was assumed to be sufficiently fast and large to handle whatever control laws were necessary to meet the handling qualities specifications. Reference 6 was to be used as a guide, with piloted simulation as a means for final refinement. The design goal was to provide constant handling characteristics throughout the flight envelope.

The control laws were initially designed in the continuous domain using classical design methods and later were converted to a discrete set.

Longitudinal Axis

Control law structure

The longitudinal axis control system is shown functionally in figure 7. The pilot's pitch stick input, δ_{e_p}, generates a normal

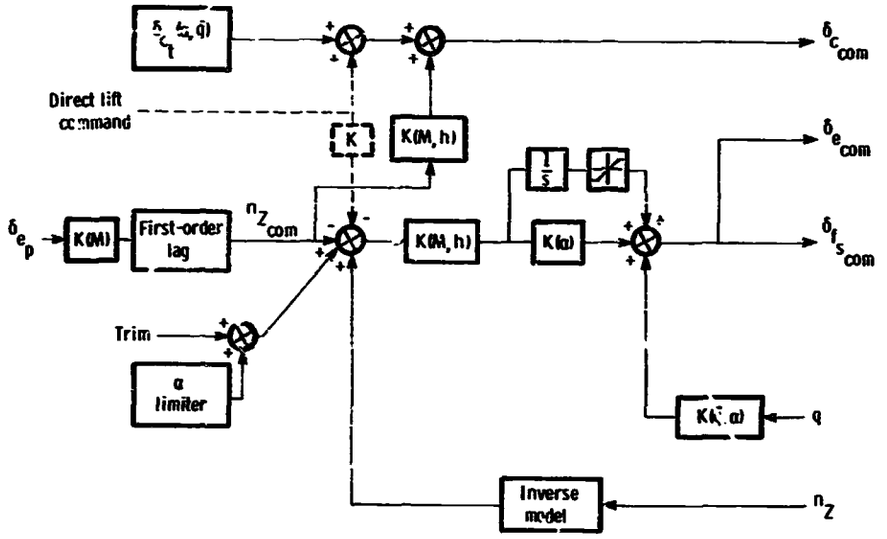

Figure 7. Longitudinal primary control law structure.

acceleration command, $n_{Z_{com}}$, through a first-order shaping filter and a gain. The value of $n_{Z_{com}}$ is compared with a filtered normal acceleration feedback, and the error is then routed through an integral-plus-proportional network in the forward loop to the elevators and symmetrical elevons. Note that many of the gains are functions of one or two variables. The forward loop gain, for example, is programed as a function of Mach number and altitude. An integral-plus-proportional network, programed as a function of angle of attack, provides neutral speed stability within the limits of the integrator limiter. Pitch rate is fed back as an inner loop to provide pitch damping. The elevators and symmetric elevons are driven in unison as the primary pitch control effectors. In the normal acceleration feedback path, an inverse model places zeros at a desirable location for the closed-loop short period to close on as the gain is increased.

A crossfeed is provided from the normal acceleration command, $n_{Z_{com}}$, to the canard. This crossfeed is needed to quicken the normal acceleration command augmentation response at high altitude, transonic flight conditions.

The angle-of-attack limiter introduces a nose down pitching moment command when a reference angle of attack, α_ℓ, is approached or exceeded. The α_ℓ is programed as a function of Mach number: At Mach 0.3, α_ℓ is equal to 10°; at Mach 0.8 and greater, α_ℓ is equal to 19°; and between these two points, α_ℓ is interpolated linearly.

The angle-of-attack limit was based on the angle of attack at which the airplane could be abruptly rolled to a 30° bank angle using the antisymmetric elevons without reaching the limits of the elevons for pitch augmentation. If an elevon reaches its limit, the symmetric elevon commands have priority over the antisymmetric elevon commands.

An attempt has been made to straighten the nonlinear $C_{m_{C_L}}$ curve by programing the canard flap as a function of angle of attack. This is reflected in the δ_{c_t}, which is only active for $M \leq 0.7$. Beginning at an angle of attack of 10°, the δ_{c_t} is a trailing edge up command proportional to the angle of attack until surface saturation is reached at an angle of attack of 16°. There is close interaction between this δ_{c_t} and the angle-of-attack limiter since they are active concurrently. The limiter begins making nose down inputs at an angle of attack of 10° to 12° for $M \leq 0.4$, whereas the canard flap makes nose down inputs at angles of attack between 10° and 16°.

Also shown in figure 7 is a separate direct lift command (dashed line) that generates a normal acceleration command, which is acted upon by the closed loop through the elevators and symmetric elevons described previously. In addition, a signal feeds directly to the canard flap.

Dynamic characteristics

As mentioned previously, an inverse model was included in the normal acceleration feedback to give a set of zeros at a desirable location for the closed-loop poles to close on. Root loci were generated by varying the normal acceleration feedback gain with the pitch rate feedback loop closed and assuming the first-order actuator lags to be 40 radians per second. Figure 8 presents a root locus for a high dynamic pressure flight condition of

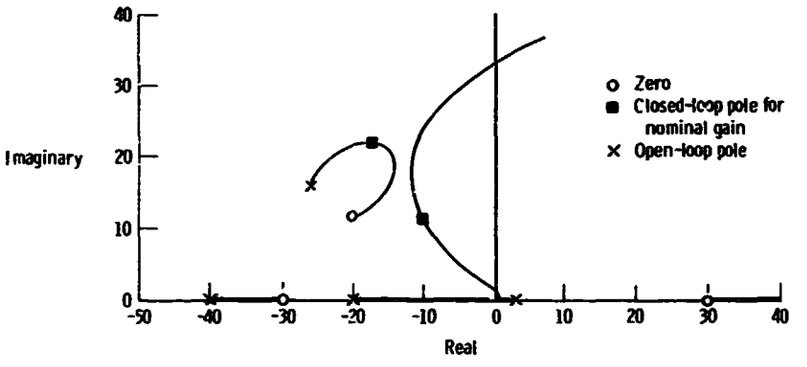

(a) Root locus.

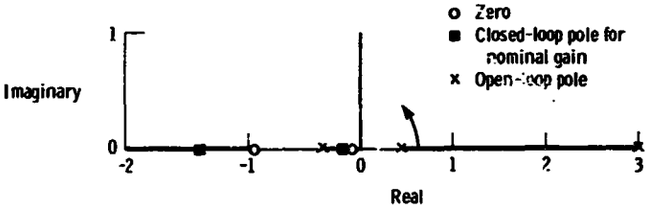

(b) Expanded view of root locus near origin.

Figure 8. Root locus for increasing normal acceleration feedback with pitch rate loop closed. Mach 0.9; h = 760 meters.

Mach 0.9 and an altitude of 760 meters. The closed-loop root locations for five representative flight conditions are shown in figure 9. The root locations and, in particular, the real zero pairs vary considerably with flight condition. Despite this variation, the dynamics of the transient response to a pilot's command is relatively invariant, even though the static response is different. An example is given in figure 10, which shows simulator time responses for identical pilot inputs at two flight conditions.

Lateral-Directional Axes

Control law structure

In the lateral-directional axes, the control laws are conventional, with the exception of an integral-plus-proportional network on lateral acceleration and the addition of a rudder pedal-to-antisymmetric elevon interconnect. Three sets of controllers are available: ailerons, antisymmetric elevons, and rudders. Figure 11 presents a block diagram of the roll-yaw normal mode control laws. As in the longitudinal axis, many of the gains are programed as functions of several variables to maintain nearly constant handling qualities.

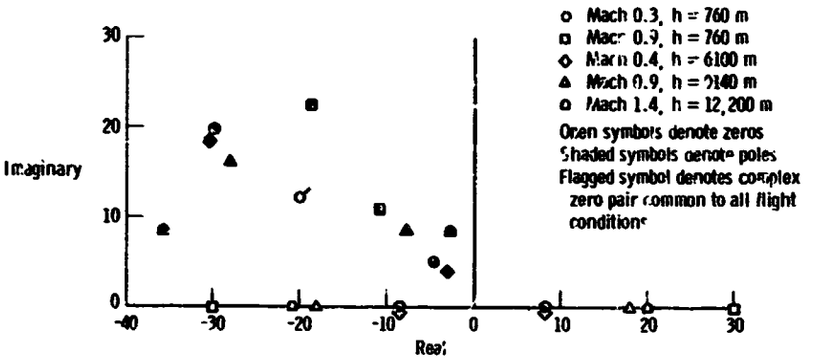

Figure 9. Closed-loop roots in longitudinal axis at selected flight conditions. Closed-loop pole-zero pairs near the origin are similar for all flight conditions.

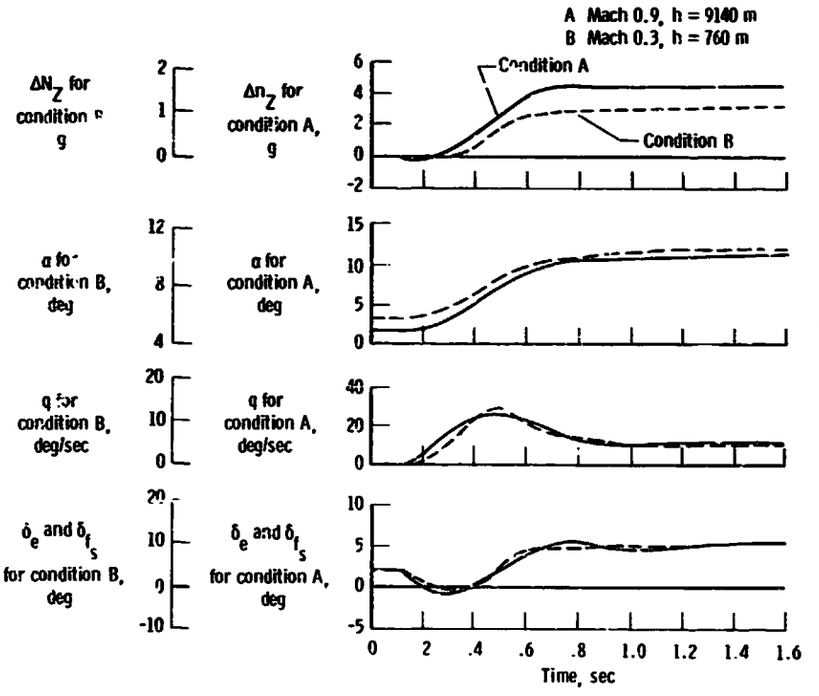

Figure 10. Time response for 3-centimeter pilot pitch stick step command at two flight conditions.

Beginning at the top half of figure 11, the pilot's roll stick signal, δ_{a_p}, is routed through a gain programed as a function of Mach number, then low passed to generate a roll rate command. The command is routed to the ailerons through a scheduled gain. The gain is constant for dynamic pressures less than 38,400 N/m^2. The gain is gradually reduced at higher dynamic pressures such that it is zero for dynamic pressures greater than 57,000 N/m^2 (aileron roll effectiveness changes sign due to flexibility at high dynamic pressure). The roll rate command is also routed to the antisymmetric elevons, which are used to augment roll damping through roll rate feedback. A roll stick-to-rudder interconnect is provided to decrease a strong adverse yaw. A lag on the interconnect with a 1-second time constant provides compatibility between the interconnect and the augmented roll subsidence mode.

Rudder pedal inputs, δ_{r_p}, are converted to directional commands in a manner similar to that for the roll stick signal. Augmentation of the Dutch roll is accomplished through lateral acceleration and yaw rate feedback. The limited integral-plus-proportional network on the lateral acceleration feedback is a direct result of the nonlinear C_{n_β} curve discussed in an earlier section. Without the integrator, directional trim may occur at non-zero angles of sideslip. With the active control philosophy, the control system is expected to provide directional trim at an angle of sideslip of 0°. If the active control system were not available, it would be necessary to stiffen the vertical tail structure to eliminate the C_{n_β} nonlinearity.

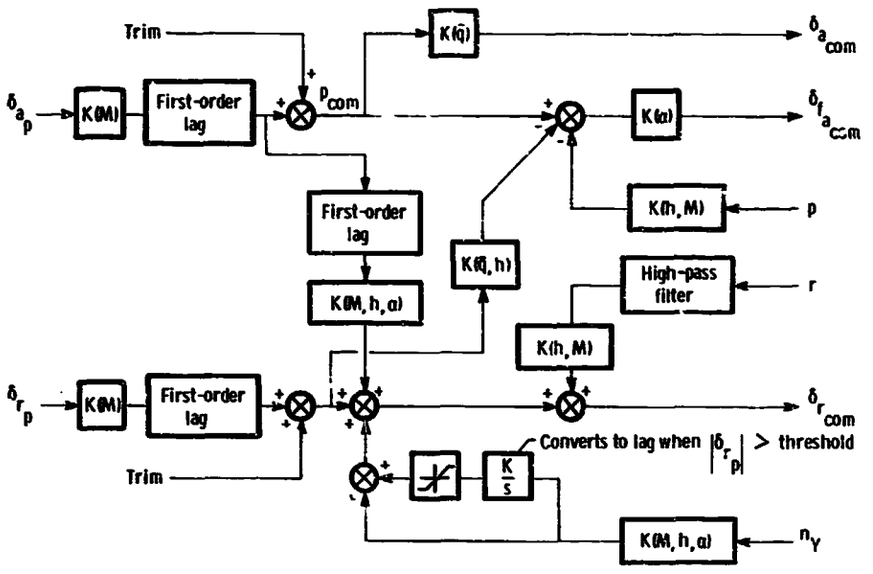

Figure 11. Lateral-directional primary control law structure.

The rudder pedal-antisymmetric elevon crossfeed is somewhat unusual in that it corrects a very minor annoyance associated with a hesitation in the lifting of the wing due to rudder pedal inputs during a crosswind approach. With a digital fly-by-wire system, corrections of minor annoyances such as this are essentially free in that the hardware is available and the impact on software is minimal.

Dynamic characteristics

The negative C_{n_β} for small angles of sideslip presents an interesting controls problem. Figure 12 shows, in root locus form, how the different augmentation loop closures change the lateral-directional dynamics. The two real, unstable roots correspond to the spiral and roll subsidence roots while the stable, oscillatory pair represent the Dutch roll roots. Note that the labeling of the roots as Dutch roll, roll subsidence, or spiral becomes difficult for these unusual, unstable configurations. The above labels were determined by the behavior of the mode shapes due to the roots, rather than by tracing the loci of roots back to their origins for a well behaved stable configuration. The initial closure, where the lateral acceleration feedback includes the integral-plus-proportional network, moves the unstable roots into the stable left half plane while decreasing the stability of the oscillatory pair. The second closure, where high-passed yaw rate is fed back, improves the damping as expected. In the final closure, the addition of the roll rate feedback improves the roll subsidence time constant by moving the real root from -2.75 to -3.95.

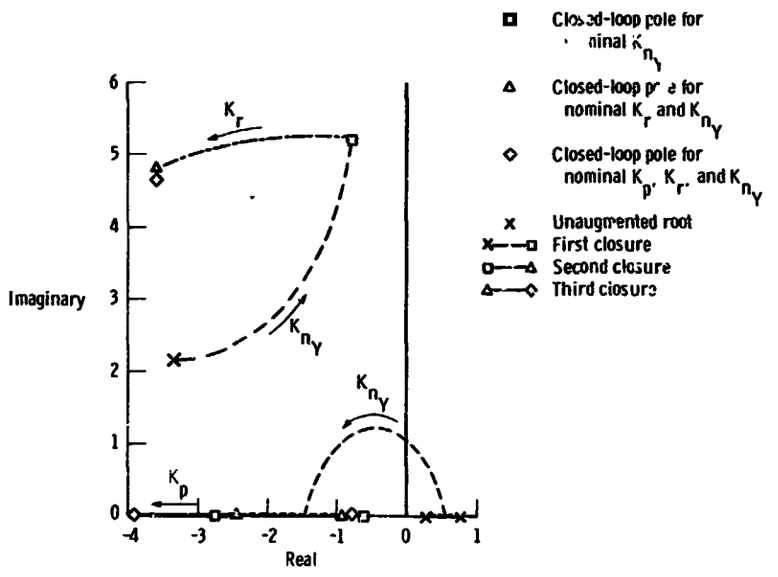

Figure 12. Effects of augmentation loop closures on the lateral-directional roots. Mach 1.0; h = 3050 meters.

Extensive programing of control system gains as functions of flight condition parameters was usually required. As an example, a comparison of the pole-zero root contours for the bank angle due to roll stick transfer function with and without gain variations with angle of attack and without roll-to-yaw interconnect is shown in figure 13. It is evident that the interconnect maintains roll control for high angles of attack; in other words, no sign change occurs in the numerator of the bank angle due to roll stick transfer functions. The angle-of-attack gain variation case shows that the zeros remain close to the corresponding poles, whereas for the fixed gain with angle of attack case, the poles and zeros become greatly separated. When the poles are close to the zeros, the roll rate response is well behaved; when the poles are well separated from the zeros, a large component of Dutch roll is present in the roll rate response.

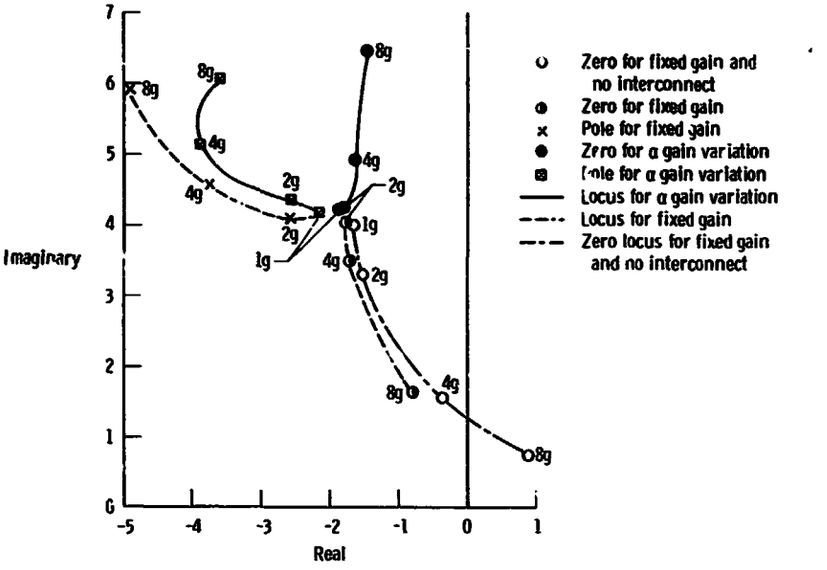

Figure 13. Effects of angle-of-attack gain schedule on bank angle due to roll stick transfer function roots.

CONTROL SYSTEM IMPLEMENTATION FOR RPRV OPERATION

The procedures followed up to this point are generally applicable to a full-scale manned aircraft. The information presented in this section, however, is unique to an RPRV operation. No attempt is made to generalize this information to a manned aircraft.

Primary Control System

Figure 14 presents a diagram of the principal elements in the control system. Separate input/output interfaces are included in each of the interfaces with the computers, although none are shown in the figure. There are three flight-safety-critical sensor sets: two within the primary system and one in the backup system. Sensor information is transmitted to the ground by way of the flight test instrumentation system. The control laws are implemented on the ground-based minicomputer, operating on the motion sensor and cockpit command information. The resulting control surface commands are transmitted to the airplane at the rate of 53.3 samples per second. Both receiver/decoders are required (eight control surface commands at four commands per unit) to transmit the commands to the primary microcomputer, which forwards the commands to the appropriate control actuators.

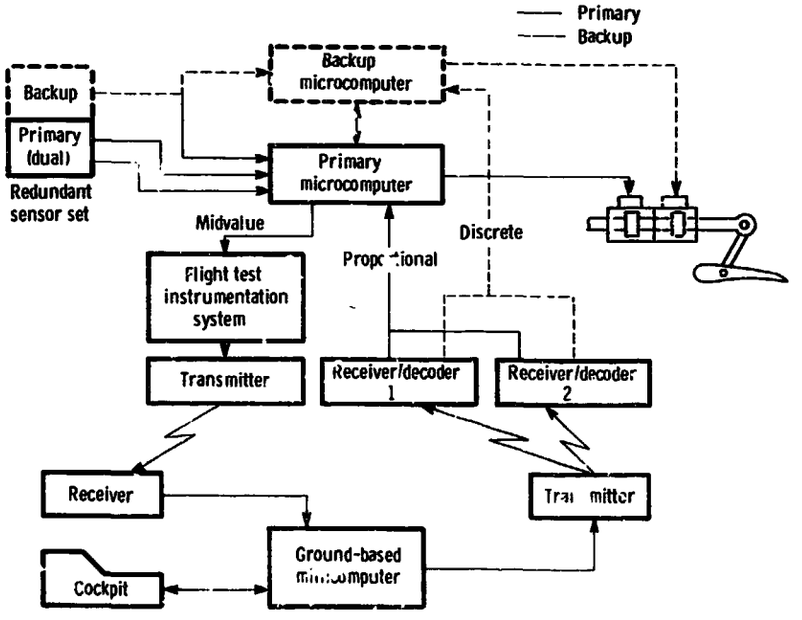

Figure 14. Arrangement of flight control system.

The control laws involve substantial use of nonlinear gain scheduling on multiple flight condition parameters. The principal elements are discussed in the following sections.

Sensor redundancy management

The flight-critical flight control sensors, the rate gyros (p, q, and r), and the normal and lateral accelerometers (n_Z and n_Y) are triplexed. The outputs of these sensors are transmitted to the primary microcomputer where the midvalue is selected. This midvalue is transmitted to the ground for primary system control loop closure. The other two values are monitored against the midvalue to within a specified tolerance for failure detection. If an out-of-tolerance condition is detected, the ground is notified as to which sensor has failed, thus aborting the mission, but the RPRV remains on the primary system.

The air data sensors (dynamic pressure, pressure altitude, and free-stream temperature) are dualized at the transducer and are designated primary and backup. A comparison is made in the primary microcomputer. When a difference greater than a prescribed level is detected, a disagreement discrete is sent to the ground. The ground-based minicomputer checks the pressure or temperature sensor information against simple models to determine which sensor has failed and switches to backup if the primary sensor has failed.

Sensors for non-flight-safety-critical parameters (bank angle, pitch attitude, heading angle, angle of attack, and angle of sideslip) are not redundant. However, the ground-based minicomputer checks these simplex sensors to determine when the data exceed reasonable limits or change at an excessive rate.

Microcomputers

The primary and backup microcomputers are based on 8080 microprocessors. Each has 1024 8-bit bytes of random access memory and provisions for 28,000 bytes of programable read-only memory (PROM). The primary microcomputer has 16,000 bytes of PROM, and the backup microcomputer has 14,000 bytes of PROM in addition to a 7-byte intercom between computers. A comprehensive self-diagnostic program runs in the background to the control software in both microcomputers. The diagnostic program includes the following tests: memory check sum, scratch pad, instruction repertoire, real-time clock accuracy, limited input/output wraparound, hardware multiplication, and computer intercom.

While in the primary system, each microcomputer carries part of the computational load. The primary microcomputer does all the datalink processing and all the failure detection for the computers, sensors, and actuators. The backup microcomputer contains the control laws for an integrated propulsion control system that replaces some of the mechanical controls on the basic J85-21 engine. It also provides backup flight control system synchroniztion information. The backup control laws do not run while on the primary system, but constants must be updated to prepare for a smooth transfer to the backup system.

Telemetry downlink and uplink

This system consists of the downlink and uplink telemetry information for control of the RPRV. The telemetry links are essentially line-of-sight transmission paths. It is estimated that flight operations will be limited to a range of approximately 60 kilometers at an altitude of 1500 meters and a range of approximately 200 kilometers at an altitude of 14,400 meters.

The downlink system provides aircraft response variables to the ground station at 220 frames per second. Approximately 2[illegible] data parameters, including 25 flight control data words, are packed into 75 words per frame. Parameters that contain useful, high frequency information are sampled at 220 samples per second; parameters of lower frequency signal content are sampled at 55 samples per second. The pulse code modulation system is a 10-bit system plus parity, although parity is not checked. A 3.7-meter parabolic receiving antenna, slaved to a radar tracking antenna, receives the transmitted signal.

The uplink system contains 16 bits per data word (a 10-bit proportional command signal and six discrete signals) Transmission is at a rate of 106.66 frames per second with four data words per frame. Since eight uplink words are required, two frames are necessary for transmission. The effective rate is 53.3 samples per second per command signal. Although two parity bits are transmitted with each word, only one bit per frame is checked by the microcomputer. A discrepancy is handled as improper information, and the system is automatically transferred to the backup mode if the discrepancy is repeated a prespecified number of times.

Ground-based minicomputer

The general purpose ground-based minicomputer has 32,000 16-bit words of memory, with a memory cycle time of 330 nanoseconds. A set of peripherals is available to support the minicomputer, including a magnetic tape drive, card reader, line printer, 2.34-million-word disc memory, and high speed paper tape reader and punch. The control laws are programed in FORTRAN IV with the input/output software written as assembly language subroutines.

Flight control surface servoactuators

Two basic types of servoactuators are used on the RPRV: fail-safe, through hydraulic locking to a predetermined or faired position; and fail-operative, through a dual-redundant (active-standby) implementation

All fail-safe simplex actuators (canards, ailerons, and elevators) use a cross-chip monitoring technique to detect failures relating to their individual channels. Since these surfaces operate either in unison or antisymmetrically from a centered position and are not mechanically interconnected, a simple comparison of their position linear voltage differential transformers (LVDT's) is used. An out-of-tolerance difference in any of the three pairs initiates a total switch to the backup system This switching is, however, reversible. In the fail-operative duplex actuators (rudder and elevon), an airborne microcomputer comparison (model) testing technique is employed. A model of the servovalve spool position is generated for comparison with the actual LVDT-measured position If the primary channel fails, the system is automatically transferred to the backup mode. This switching is reversible if the failure disappears.

Backup Control System

The backup control system was designed to recover and return the vehicle to a stable attitude after a primary system failure; place the vehicle in a constant bank angle orbit mode until commanded to exit orbit; permit remote control of the vehicle from the ground or a chase aircraft by discrete command; provide emergency landing capability; and provide a glide mode for the best range with the engine out.

Functional description

The above functions could be accomplished through the use of only the elevons, rudders, and throttle. An autopilot was designed with the nine operating modes described below.

The RECOVER mode returns the vehicle to a stable attitude after a switch to the backup system. Although the attitude gyros are not required, they are used to update the direction cosines, which are used to transform rate gyro outputs to attitude signals. Once recovery is complete, the system automatically switches to the ORBIT mode. The RPRV climbs or descends to a preespecified altitude, maintaining a constant turn rate.

Either the ground station or the chase airplane can initiate the EXIT ORBIT mode. The RPRV then goes to wings-level flight, maintains altitude, and automatically transfers to the STRAIGHT AND LEVEL mode. This mode maintains a straight track on the last heading and holds attitude. The DIVECLIMB and TURN modes may be commanded by the pilot to dive or climb at a predetermined, altitude-dependent altitude rate, or to turn at a bank angle of 35°.

Landing can be initiated by either command station by transferring to the LANDING mode. An altitude rate of descent, which is a function of radar altitude, is then maintained by the autopilot. The altitude rate can be modified by the pilot. A MACH COMMAND mode is also selectable for assisting with speed control during the landing approach.

If the engine is out, the ENGINE OUT mode is automatically selected. The pilot can make discrete speed changes and has access to the TURN MODE to make heading changes.

Implementation

The backup system uses sensors that are part of the redundant sets discussed previously and shown in figure 14. One sensor of each set is designated the backup sensor. If the backup sensor is in a triplex set, it is routed to both microcomputers. If the backup sensor is in a duplex set, it is connected only to the backup microcomputer. The primary microcomputer receives the backup sensor information indirectly through the computer intercom from the backup microcomputer. In either case, the backup microcomputer receives the backup sensor data directly.

The backup microcomputer accomplishes all necessary processing while in the backup mode. It processes all the uplinked discrete commands, the full set of backup control laws, and a subset of the integrated propulsion control system control laws. If the primary microcomputer is operable, it continues to process downlink data and a subset of failure detection software.

The rudder and elevon servoactuators are fail-operative, active-standby devices as described previously. The standby channels are switched on if transfer is made to the backup system.

Through a set of toggle switches, either the ground cockpit or a chase airplane can command mode changes within the backup system. The ability to make discrete changes to the altitude rate schedule in the LANDING mode is also provided at these command stations. The commands are in the form of discretes received by either receiver/decoder. A full set of commands can be received even if one of the receiver/decoders has failed.

CONCLUDING REMARKS

The design of a HiMAT RPRV has been completed, with active controls, a major new technology, incorporated in the design. The HiMAT RPRV is part of a new method for bringing advanced aircraft technologies to a state of readiness. The method involves the design and flight test of an RPRV based on a full-scale manned vehicle design incorporating the technologies of interest.

An examination of the active controls design process that resulted in the HiMAT RPRV reveals the following factors, which probably have general applicability to the design of full-scale operational airplanes of similar planform:

1. The active controls design process differed from conventional design processes in that although the control power sizing requirements were needed at the start of the design iteration, sufficient information to make such specifications were only available at the completion of the iteration. Better rough order-of-magnitude guidelines are needed to begin the iteration cycle.

2. Although a maximum of 10-percent negative static margin was used as a guideline for relaxed longitudinal stability and was increased to 15 percent later, nonlinearities in $C_{m_{C_L}}$ led to more than 30-percent negative static margin for some high angle-of-attack flight conditions at low Mach numbers. As a result, an angle-of-attack limiter was required to assure adequate excess control authority to stabilize the aircraft.

3. Neutral directional stability was selected as a limit for the rigid airplane. However, flexibility effects caused negative stability for small angles of sideslip. A relaxed directional static stability system was required with special provisions to prevent trimming to nonzero angles of sideslip.

4. Some penalties were incurred because of the active control functions. Actuators and hydraulic systems were larger than those required for an aircraft of conventional design. Installation of some actuators outside the wing mold line was required. Use of canard flaps to generate direct side force led to increased canard dihedral, and the addition of wingtip ventrals was necessary to compensate for the destabilizing canard dihedral effect.

5. Direct lift was provided by the canard flap and wing trailing edge surfaces' working together. The active control system deflects the wing trailing edge surfaces to counteract the nose up pitching moment due to a downward canard flap deflection. This effectively increases wing camber without inducing a net aircraft pitching moment, resulting in direct lift.

6. The primary control system was designed under the assumption that a full-time digital fly-by-wire system was available to interconnect the pilot's commands and the motion sensors with all the control surface actuators. The resulting control laws involved substantial scheduling of nonlinear gains as functions of multiple flight condition parameters.

Although the control system implementation for RPRV operation cannot be generalized to an operational piloted airplane, a versatile system suitable for remotely piloted flight research was defined. The system makes effective use of a ground-based minicomputer and two onboard microcomputers.

REFERENCES

1. Lockenour, Jerry L.; and Layton, Garrison P.: RPRV Research Focus on HiMAT. Astronaut. & Aeronaut., Apr. 1976, pp. 36-41.

2. Rynaski, Edmund G.; and Weingarten, Norman C.: Flight Control Principles for Control Configured Vehicles. Air Force Flight Dynamics Lab., AFFDL-TR-71-154, Wright-Patterson Air Force Base, Jan. 1972.

3. Berger, R. L.; Hess, J. R.; and Anderson, D. C.: Compatibility of Maneuver Load Control and Relaxed Static Stability Applied to Military Aircraft. AFFDL-TR-73-33, Air Force Flight Dynamics Lab., Wright-Patterson Air Force Base, Apr. 1973.

4. Edwards, John W.; and Deets, Dwain A.: Development of a Remote Digital Augmentation System and Application to a Remotely Piloted Research Vehicle. NASA TN D-7941, 1975.

5. Crother, C. A.; Abramson, R.; and Speyer, E. N.: Analysis of Relaxed Static Stability and Maneuver Load Control Applications to a Large Bomber. AFFDL-TR-72-7, Air Force Flight Dynamics Lab., Wright-Patterson Air Force Base, Feb. 1972.

6. Flying Qualities of Piloted Airplanes. Military Specification MIL-F-8785B(ASG), Aug. 7, 1969.

ACKNOWLEDGMENT

The authors are indebted to Marshall Roe of Rockwell International for his contributions concerning the aerodynamic configuration development experience with the HiMAT RPRV.